Supplementary Information for A Giant Thermal Switching in Ferromagnetic VSe_2 with Programmable Switching Temperature

Chao Wu,[a, b] Yunshan Zhao,[c] Gang Zhang,[*, d] Chenhan Liu[*, a, e]

[a] *Micro- and Nano-scale Thermal Measurement and Thermal Management Laboratory, School of Energy and Mechanical Engineering, Nanjing Normal University, Nanjing, 210046, P. R. China*

[b] *Jiangsu Key Laboratory for Design and Manufacture of Micro-Nano Biomedical Instruments, School of Mechanical Engineering, Southeast University, Nanjing, 211100, P. R. China.*

[c] *NNU-SULI Thermal Energy Research Center (NSTER) & Center for Quantum Transport and Thermal Energy Science (CQTES), School of Physics and Technology, Nanjing Normal University, Nanjing 210023, P. R. China*

[d] *Institute of High Performance Computing, Agency for Science, Technology and Research, 138632, Singapore*

[e] *Jiangsu Key Laboratory for Numerical Simulation of Large-Scale Complex Systems, Nanjing Normal University, Nanjing, 210046, P. R. China*

***Corresponding authors:** chenhanliu@njnu.edu.cn; zhangg@ihpc.a-star.edu.sg

Supplementary Note 1

The first-principles calculation details

The phonon dispersion and phonon density of states (DOS) are calculated in Phonopy package.[1] The specific heat, phonon group velocity, weighted phonon-phonon scattering phase space, phonon-phonon scattering rates, thermal conductivity, and Grüneisen parameter are calculated in ShengBTE package.[2] The relaxed structure, second-order force constant, and third-order force constant needed by above two packages are calculated in Vienna Ab-initio Simulation Package (VASP).

The structure relaxation with (FM) and without (PM) spin polarization is performed in VASP with 19×19×1 K point mesh for monolayer VSe_2 (11×11×5 for bulk counterpart) and force tolerance of 0.005 eV/Å. The energy cut off of the plane wave basis set is 500 eV with the projector augmented wave (PAW) pseudopotentials.[3]

The generalized gradient approximation (GGA) of Perdew-Burke-Ernzerhof (PBE) is applied for the electronic exchange-correlation functional. In order to describe the interlayer van der Waals interaction, DFT-D3 method is applied. A 5×5×1 supercell with 5×5×1 K point mesh and a 4×4×3 supercell with 1×1×1 K mesh are applied to calculate second-order force constant for monolayer and bulk VSe_2, respectively. A 6×4×1 supercell with 3×3×1 K point mesh and a 3×3×2 supercell with 2×2×2 K point mesh are applied to calculate third-order force constant for monolayer and bulk VSe_2, respectively. The cutoff is set as 0.65 nm for third-order force constant calculations.

Under the framework of linearized Boltzmann transport equation, the thermal conductivity k can be calculated as following:[2]

$$k_{\alpha\beta} = \frac{1}{k_B T^2 \Omega N} \sum_{\lambda} f_0 (f_0 + 1) (\hbar\omega)^2 v_\lambda^\alpha v_\lambda^\beta \tau_\lambda \tag{S1}$$

$$\frac{1}{\tau_\lambda} = \frac{1}{N} \left(\sum_{\lambda' \lambda''}^{+} \Gamma^{+}_{\lambda \lambda' \lambda''} + \frac{1}{2} \sum_{\lambda' \lambda''}^{-} \Gamma^{-}_{\lambda \lambda' \lambda''} + \sum_{\lambda'} \Gamma_{\lambda \lambda'} \right) \tag{S2}$$

$$\Gamma^{+}_{\lambda \lambda' \lambda''} = \frac{\hbar\pi \left(f_0' - f_0'' \right)}{4 \omega_\lambda \omega_{\lambda'} \omega_{\lambda''}} \left| V^{+}_{\lambda \lambda' \lambda''} \right|^2 \delta \left(\omega_\lambda + \omega_{\lambda'} - \omega_{\lambda''} \right) \tag{S3}$$

$$\Gamma^{-}_{\lambda \lambda' \lambda''} = \frac{\hbar\pi \left(f_0' + f_0'' + 1 \right)}{4 \omega_\lambda \omega_{\lambda'} \omega_{\lambda''}} \left| V^{-}_{\lambda \lambda' \lambda''} \right|^2 \delta \left(\omega_\lambda - \omega_{\lambda'} - \omega_{\lambda''} \right) \tag{S4}$$

Where α (β) denotes the direction x or y or z, k_B is Boltzmann constant, T is temperature, Ω is the volume of unit cell shown in Fig. 1, N is the number of phonon modes λ including phonon wavevector and branch, f_0 is equilibrium phonon distribution, $\hbar$ is the reduced Planck constant, ω is the phonon angular frequency, v is the phonon group

velocity, τ is phonon lifetime and V is the scattering matrix element.[4, 5] The quantities Γ in equations (S3) and (S4) are phonon-phonon scattering rates and the superscripts "+" and "-" mean the adsorption and emission processes respectively. The Dirac delta functions inside the expressions of Γ mean the energy should be conserved during phonon-phonon scattering process. The conservation of quasi-momentum is not clearly shown here. Actually, the phonon mode λ'' in equations (S3) and (S4) is determined under the condition of quasi-momentum conservation $\lambda'' = \lambda \pm \lambda' + G$, where G is the reciprocal lattice vector and the symbol " $\pm$ " has same meaning as above.

In order to describe FM orderings effects on phonon-phonon scattering, the weighted phonon-phonon scattering phase space WP3 is calculated and written as:[6, 7]

$$W_{\lambda}^{\pm} = \frac{1}{2N}\sum_{\lambda'\lambda''}\begin{Bmatrix} 2(f_{\lambda'} - f_{\lambda''}) \\ f_{\lambda'} + f_{\lambda''} + 1 \end{Bmatrix}\frac{\delta(\omega_{\lambda} \pm \omega_{\lambda'} - \omega_{\lambda''})}{\omega_{\lambda}\omega_{\lambda'}\omega_{\lambda''}} \quad \text{(S5)}$$

Where the symbols have the same physical meanings as above. The upper part in the bracket means the absorption process while the lower part means the emission process. By comparing equations (S3) or (S4) and (S5), the weighted scattering phase space describes the allowed number of phonon-phonon scattering channels.

A 60×60×1 ***q***-mesh with a scalebroad of 1.0 for monolayer 2H-VSe_2 (a 21×21×7 ***q***-mesh with a scalebroad of 1.0 for bulk counterpart) is chosen to calculate the thermal conductivity. To guarantee the convergence of calculations, different ***q***-mesh (the number of ***q*** pints) and scalebroad (Gaussian width) are tested in FM monolayer 2H-VSe_2 and shown in Fig. S4. From the figure, 60×60×1 ***q***-mesh is large enough to

guarantee the convergence and scalebroad of 1.0 is also well enough. In addition, the isotope scattering is considered and BTE is iteratively solved.

Supplementary Note 2

The magnetic transition temperature calculation of bulk 2H-VSe_2

To evaluate the strength of spin interactions between V atoms in monolayer VX_2, the parameters J in spin Hamiltonian is derived. Based on the Heisenberg model,[8] the spin Hamiltonian is described as $H = -J\sum_i \sigma_i\sigma_{i+1}$, where σ_i is the net spin induced by the i^{th} V atom site. Based on the model, the energy difference ΔE between the AFM and FM phases is $E^{AFM} - E^{FM} = 2J|\sigma_i|^2$,[9, 10] from which the energy of exchange interactions J can be obtained. The Curie temperature can be simply estimated by J/k_B,[10] where k_B is the Boltzmann constant. The J of bulk VSe_2 is 7.17 meV and the Curie temperature is estimated about 80 K.

The mode dependent phonon group velocity

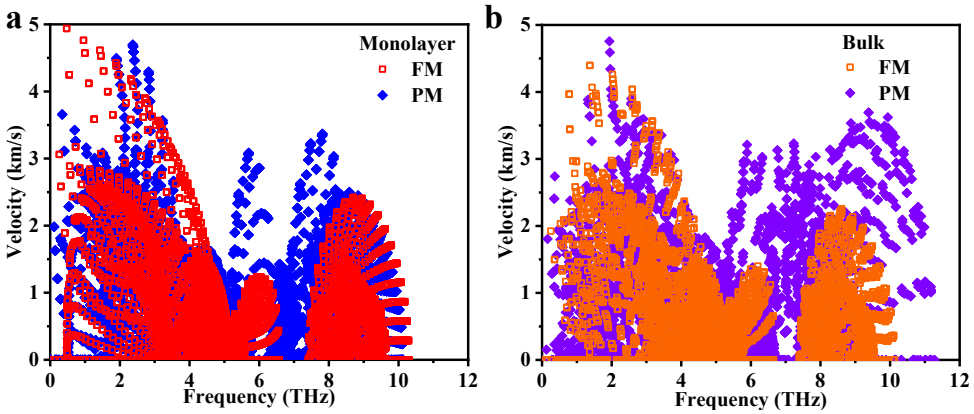

Fig. S1 The mode (frequency) dependent phonon group velocity of monolayer (a) and bulk (b) 2H-VSe_2 at the magnetic transition temperature from FM (hollow symbols) to PM (solid symbols) phase.

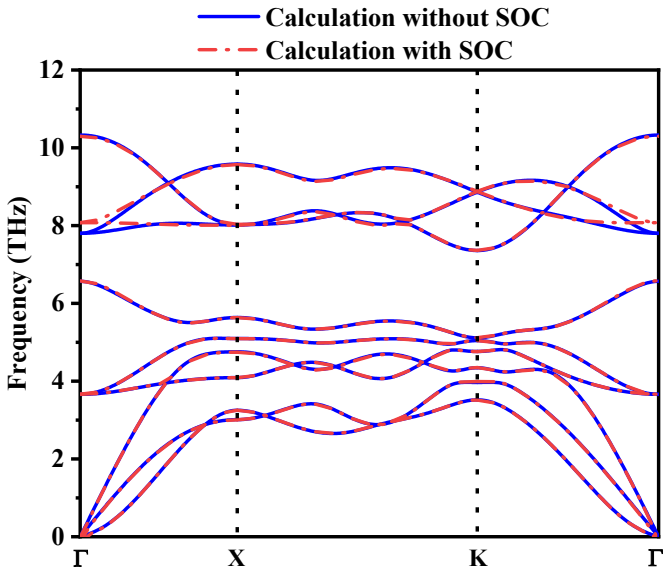

Fig. S2 Phonon dispersion of monolayer FM 2H-VSe_2 with (red dotted lines) or without (blue lines) introducing spin-orbit coupling.

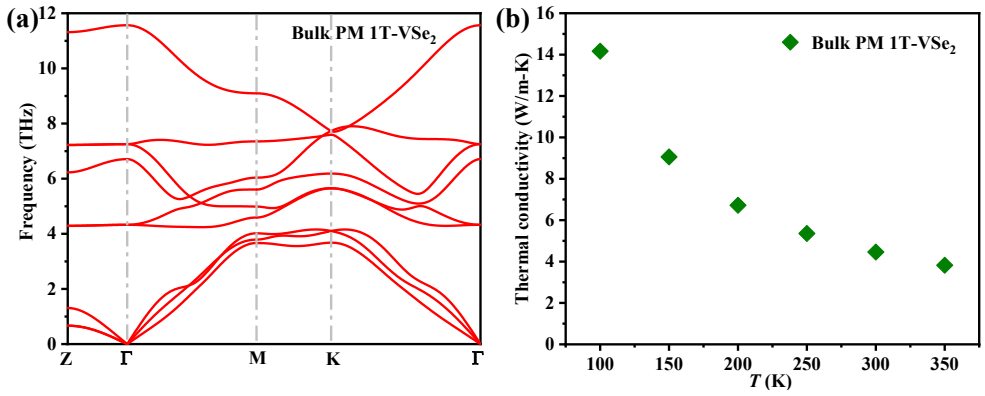

Fig. S3 Phonon dispersion (a) and thermal conductivity (b) of bulk PM 1T-VSe_2. Since the experimental thermal conductivity of 2H-VSe_2 is still lacking, our calculated value of 4.5 W/m-K for bulk 1T-VSe_2 at room temperature is consistent with previous experimental measurement,[11] indicating the accuracy of our calculations.

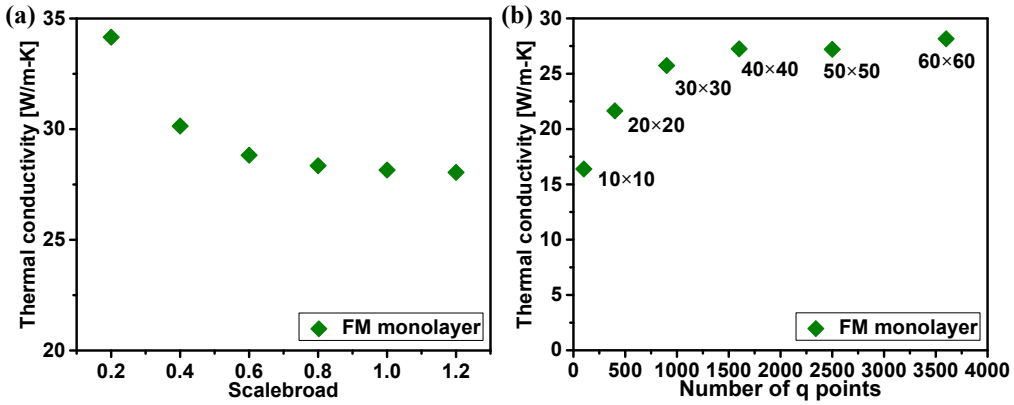

Fig. S4 Scalebroad and number of q points dependent thermal conductivity in FM monolayer 2H-VSe_2 at 430 K.

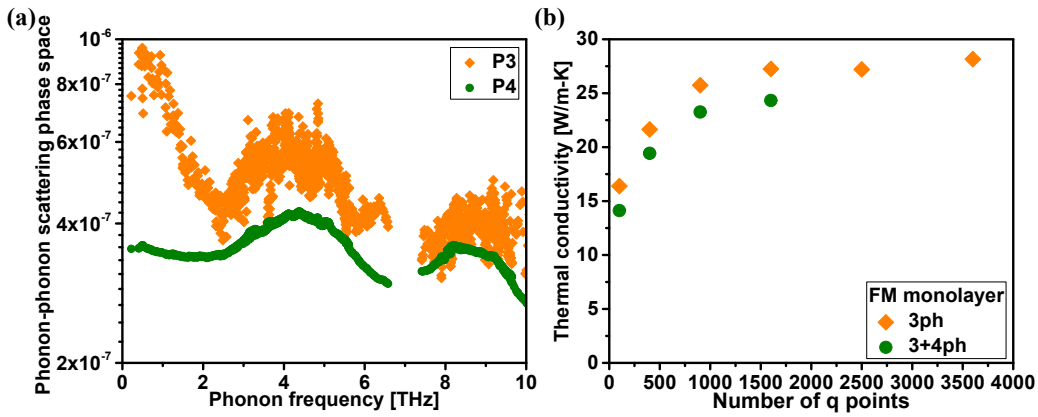

Fig. S5 (a) Phonon frequency dependent three-phonon scattering phase space (P3) and four-phonon scattering phase space (P4) of monolayer FM 2H-VSe_2 at 430 K. (b) Number of q points dependent thermal conductivity for three-phonon and both three- and four-phonon process at 430 K. The calculated thermal conductivity with both three- and four-phonon process is about 10% smaller than that with only three-phonon process at 430 K for monolayer FM 2H-VSe_2. Thus, the four-phonon process is not that important in 2H-VSe_2.

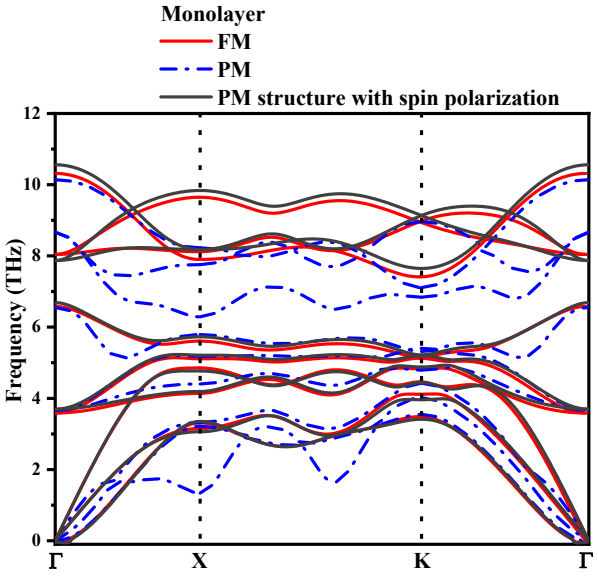

Fig. S6 Phonon dispersion of monolayer FM phase (red lines), PM phase with (black lines) or without spin polarization (blue dotted lines). The phonon dispersion of PM structure with spin polarization is similar to that of FM structure but much different to that of PM structure without spin polarization, indicating that the large thermal conductivity variation in 2H-VSe_2 is caused by magnetic order while structural change has weak effects.

The lattice parameters of VSe_2

Table S1. The lattice parameters of monolayer and bulk VSe_2 in PM and FM phases, respectively.

Thickness	Lattice parameters	PM	FM	Side view of the structure
Monolayer	a, b (Å)	3.30863	3.32720	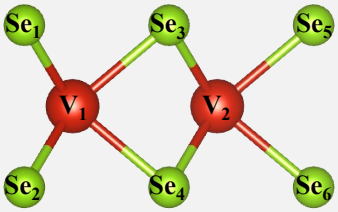
		-	3.326[12]	
		-	3.33[13]	
	V_1-Se_{1-4} (Å)	2.49029	2.50182	
	V_1-V_2 (Å)	3.30863	3.32720	
	$\angle Se_1V_1Se_2$	79.8164°	79.6823°	
	$\angle Se_3V_1Se_4$	79.8164°	79.6823°	
	$\angle Se_1V_1Se_3$	83.2581°	83.5770°	
	***E* (eV)**	-18.5490	-18.6301	
Bulk	a (Å)	3.30695	3.32407	

		-	3.319[12]	
		-	3.17[13]	
	c (Å)	12.59932	12.71758	
		-	12.817[12]	
		-	12.13[13]	
	V_1-Se_{1-4} (Å)	2.48355	2.49408	
	V_1-V_2 (Å)	3.30622	3.32342	
	$\angle Se_1V_1Se_2$	79.5332	79.4029	
	$\angle Se_1V_1Se_3$	83.4607	83.5585	
	***E* (eV)**	-37.6717	-37.7931	

References

1. A. Togo and I. Tanaka, *Scripta Mater.*, 2015, **108**, 1-5.
2. W. Li, J. Carrete, N. A. Katcho and N. Mingo, *Comput. Phys. Commun.*, 2014, **185**, 1747-1758.
3. G. Kresse and D. Joubert, *Phys. Rev. B*, 1999, **59**, 1758-1775.
4. A. Ward, D. A. Broido, D. A. Stewart and G. Deinzer, *Phys. Rev. B*, 2009, **80**, 125203.
5. L. Lindsay and D. A. Broido, *J. Phys-Condens Mat.*, 2008, **20**, 165209.
6. W. Li and N. Mingo, *Phys. Rev. B*, 2014, **89**, 184304.
7. W. Li and N. Mingo, *Phys. Rev. B*, 2015, **91**, 144304.
8. W. Nolting and A. Ramakanth, *Heisenberg Model*, Quantum Theory of Magnetism. Springer, Berlin, Heidelberg, 2009: 273-386.
9. Y. Ma, Y. Dai, M. Guo, C. Niu, Y. Zhu and B. Huang, *Acs Nano*, 2012, **6**, 1695-1701.
10. H. R. Fuh, C. R. Chang, Y. K. Wang, R. Evans, R. W. Chantrell and H. T. Jeng, *Sci Rep-Uk*, 2016, **6**, 32625.
11. S. Wang, R. Wang, L. Wang and J. Chang, *Solid State Commun.*, 2020, **318**, 113983.
12. H. R. Fuh, B. H. Yan, S. C. Wu, C. Felser and C. R. Chang, *New J. Phys.*, 2016, **18**, 113038.
13. A. H. M. A. Wasey, S. Chakrabarty and G. P. Das, *J. Appl. Phys.*, 2015, **117**, 064313.